Singly and doubly lithium doped silicon clusters: Geometrical and electronic structures and ionization energies

Nguyen Minh Tam, Vu Thi Ngan, Jorg de Haeck, Soumen Bhattacharyya, Hai Thuy Le et al.

Citation: J. Chem. Phys. **136**, 024301 (2012); doi: 10.1063/1.3672164
View online: http://dx.doi.org/10.1063/1.3672164
View Table of Contents: http://jcp.aip.org/resource/1/JCPSA6/v136/i2
Published by the American Institute of Physics.

Singly and doubly lithium doped silicon clusters: Geometrical and electronic structures and ionization energies

Nguyen Minh Tam,[1,2] Vu Thi Ngan,[1] Jorg de Haeck,[3] Soumen Bhattacharyya,[3] Hai Thuy Le,[3] Ewald Janssens,[3] Peter Lievens,[3,a)] and Minh Tho Nguyen[1,b)]
[1]*Department of Chemistry, Katholieke Universiteit Leuven, B-3001 Leuven, Belgium*
[2]*Institute for Computational Science and Technology, Ho Chi Minh City, Vietnam*
[3]*Laboratory of Solid State Physics and Magnetism, Katholieke Universiteit Leuven, B-3001 Leuven, Belgium*

(Received 24 October 2011; accepted 5 December 2011; published online 9 January 2012)

The geometric structures of neutral and cationic $Si_nLi_m^{0/+}$ clusters with $n = 2$–11 and $m = 1$, 2 are investigated using combined experimental and computational methods. The adiabatic ionization energy and vertical ionization energy (VIE) of Si_nLi_m clusters are determined using quantum chemical methods (B3LYP/6-311+G(d), G3B3, and CCSD(T)/aug-cc-pVxZ with x = D,T), whereas experimental values are derived from threshold photoionization experiments in the 4.68–6.24 eV range. Among the investigated cluster sizes, only Si_6Li_2, Si_7Li, $Si_{10}Li$, and $Si_{11}Li$ have ionization thresholds below 6.24 eV and could be measured accurately. The ionization threshold and VIE obtained from the experimental photoionization efficiency curves agree well with the computed values. The growth mechanism of the lithium doped silicon clusters follows some simple rules: (1) neutral *singly doped* Si_nLi clusters favor the Li atom addition on an edge or a face of the structure of the corresponding Si_n^- anion, while the cationic Si_nLi^+ binds with one Si atom of the bare Si_n cluster or adds on one of its edges, and (2) for *doubly doped* $Si_nLi_2^{0/+}$ clusters, the neutrals have the shape of the Si_{n+1} counterparts with an additional Li atom added on an edge or a face of it, while the cations have both Li atoms added on edges or faces of the Si_n^- clusters. © *2012 American Institute of Physics*. [doi:10.1063/1.3672164]

I. INTRODUCTION

Silicon-based clusters have received continuing attention in part due to their numerous technological applications and the intensive ongoing efforts to reduce sizes in nanomaterials.[1–12] However, the determination of the ground state structure of clusters is not straightforward and remains a challenging subject. Structures of small neutral and positively charged silicon clusters, predicted earlier by theory, have only recently been confirmed or clarified by far-infrared spectroscopic experiments.[13,14] Due to the small 3*s*–3*p* energy gap of the Si atom, silicon clusters favor structures where the Si atoms have tetrahedral hybridization rather than triangular hybridization as carbon in fullerenes. Therefore, fullerene-like Si clusters, which may be obtained by proper metal doping,[15–17] remain elusive targets. Since the first experimental realization of transition metal doping,[18] much effort has been devoted to the search for dopants that trigger the formation of endohedral high-symmetric silicon clusters. In this context, the study of the structure of doped silicon clusters provides fundamental knowledge needed for their potential use in new materials and applications.

Transition metal atoms can be encapsulated in a Si cage consisting of 11 or 12 Si atoms onward. Smaller main element atoms can even be placed inside a smaller sized cage. For example, the Be atom is found to be able to locate at the center of a Si_8 cube, while the Li^- anion is not.[19] Using *ab initio* molecular dynamics simulations Majumder and Kulshreshtha[20] showed that Be and B atoms are encapsulated in a bicapped tetragonal prism Si_{10}, while Li, Na, Mg, and Al prefer to expose on the surface of the clusters.

Previous studies demonstrated that Li behaves as an electron donor in neutral Si_nLi.[21–24] Hence, the Li atom favors adsorption on a bridge site of the corresponding Si_n cluster and the silicon framework in Si_nLi species is basically similar to that of the Si_n^- anion.[21] Using the G3 technique to probe the structures of the small neutral and anionic $Si_nLi^{0/-}$ (n = 1–8) series, Yang *et al.*[25] found that the ground state structures of neutral Si_nLi are of adsorptive type in which Li is simply added to the Si_n clusters, whereas the Si_nLi^- anions are of substitutional type. Logically, one adsorptive Li atom and one substitutional Li atom could be expected in the doubly doped neutral Si_nLi_2 clusters. However, Sporea *et al.*[22,24] did not come to that conclusion in a theoretical study on structures of small Si_nLi and Si_nLi_2 (n = 1–6). These authors deduced that even in Si_nLi_2, the bare Si_n frames remain and both Li atoms act as electron donors. A similar behavior was found for sodium doped Si_nNa_m clusters ($n \leq 6$; $m \leq 2$).[26] This finding may not be generalized because the authors only considered small silicon clusters. It is apparent that larger singly and doubly lithium-doped silicon cluster sizes should carefully be investigated before a general growth pattern can be established. A few small mixed lithium-silicon clusters with more than two Li atoms were also studied theoretically.[27] Interestingly, the multi-lithium doped silicon cluster $Si_5Li_7^+$

a)Electronic mail: peter.lievens@fys.kuleuven.be.
b)Electronic mail: minh.nguyen@chem.kuleuven.be.

was predicted to have a perfect seven-peak star-like structure due to the electron donation behavior of the Li atoms.[28] Some experimental data on sodium doped silicon clusters, including threshold photoionization and photoelectron spectroscopy studies, are available.[29–32] However, not many experiments are reported for the lithium congener.

Measurements of the ionization energy (IE) of silicon clusters are limited by the availability of tabletop tunable laser light sources, which provide sufficiently short wavelengths. Therefore, only recently the IEs of small silicon clusters (Si_n, $n = 1$–7) could be measured using vacuum ultraviolet light of a synchrotron with relatively high accuracy.[33] In a forthcoming article,[34] we describe in detail the measurements of the photoionization efficiency (PIE) curves of Si_nLi_3 ($n = 5$–11) and Si_8Li_m ($m = 3$–6), which makes available both vertical IE (VIE) and adiabatic IE (AIE) for these mixed lithium-silicon clusters with a high accuracy.

In the present paper, the geometrical and electronic structures and energetics of the singly and doubly lithium doped silicon clusters in both neutral and cationic states, $Si_nLi_m^{0/+}$ with $n = 1$–11 and $m = 1$–2, are discussed. The theoretical investigation is carried out in concert with the experimental threshold photoionization measurements. However, among the investigated species only Si_6Li_2, Si_7Li, $Si_{10}Li$, and $Si_{11}Li$ have sufficiently low ionization thresholds allowing experimental determination of their ionization energies. Our ultimate goal is to identify the ground state structure of the clusters and to derive the role of the lithium atoms upon investigation of their growth mechanisms in comparison with the bare silicon clusters.

II. EXPERIMENTAL METHODS

The Si_nLi_m clusters are produced in a pulsed dual-target laser vaporization source, described in detail elsewhere.[35] Two rectangular targets of silicon and lithium are ablated by focused 532 nm Nd:YAG laser light and energy densities of 8.0 and 0.2 mJ/cm^2, respectively. The cluster source produces particles in the cationic and anionic charge states, as well as neutral clusters. Charged clusters, as produced in the source, are electrostatically deflected to investigate the neutral clusters. Post-ionization is, however, required to detect the neutral clusters and to record a mass spectrum using a reflectron time-of-flight mass spectrometer. Typical mass abundance spectra of neutral Si_nLi_m obtained by post-ionization are shown in Fig. 1 using either 7.89 eV (F_2 excimer laser) or 6.42 eV laser light (ArF excimer laser). The laser energy density is kept low to ensure that no significant amount of photon induced fragmentation takes place.

Certain cluster sizes appear to be more abundant in Fig. 1(a), which is recorded with 6.42 eV photons. Enhanced intensities are recorded for Si_5Li_3, Si_6Li_2, Si_7Li_1, and Si_9Li_5. However, one cannot directly relate enhanced abundances to enhanced stabilities. The recorded intensity not only depends on the abundance in the cluster beam but also on the ionization efficiency. This is clearly illustrated by the high abundances of Si_nLi_2 clusters in the mass spectrum, as shown in Fig. 1(b), recorded after ionization with a photon energy of 7.89 eV, while they are almost absent in Fig. 1(a). Previous

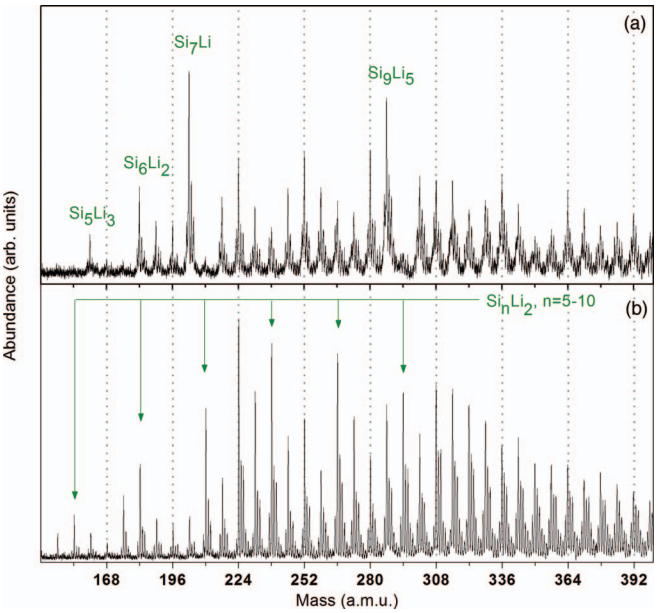

FIG. 1. Mass abundance spectra of neutral Si_nLi_m clusters produced at 100 K and post-ionized using either (a) 6.42 eV photons or (b) 7.89 eV photons. The green arrows mark Si_nLi_2 and dotted lines the bare Si_n clusters.

threshold ionization measurements revealed that the Si_n clusters with $n = 1$–7 and 10 have an ionization threshold above 7.89 eV (Ref. 36), and thus their recorded intensities do not reflect their abundance in the cluster beam. For a correct interpretation of the mass spectrum of neutral clusters, the ionization efficiency of each cluster must be known.

In the forthcoming article,[34] we describe in detail the measurements of the PIE curves of Si_nLi_m. Briefly, the neutral clusters are ionized by tunable laser light from a dye laser and PIE curves are obtained for each size by scanning the ionization laser in a range from 4.68 to 6.24 eV with a step size of 0.04 eV. Each data point is measured multiple times and is normalized by a reference value taken at the photon energy of 6.42 eV. Both the ionization threshold and the VIE are derived by fitting a smeared out step function onto the experimental data.[34] Basically, it is assumed that both the neutral and the ionic cluster can be described by harmonic potentials with the same vibrational frequency that photoionization from a specific initial vibrational state to a specific final vibrational state is a step function, and that one can neglect temperature effects. Under these conditions the VIE corresponds to the maximum increase in the ion signal (the maximum of the first derivative of the PIE curve).[37]

Of all singly and doubly lithium doped silicon clusters in the considered mass range, i.e., $Si_nLi_{1,2}$ with $n \leq 11$, only Si_7Li, $Si_{10}Li$, $Si_{11}Li$, and Si_6Li_2 have ionization energies in the studied energy range ($\leq$6.24 eV). The ionization threshold of the other $Si_nLi_{1,2}$ ($n \leq 11$) species is above 6.24 eV. All of them show up intensely in the mass spectrum measured using 7.89 eV photons (Fig. 1(b)), which puts an upper limit on their ionization threshold.

Fig. 2 shows the PIE curves of Si_7Li, $Si_{10}Li$, $Si_{11}Li$, and Si_6Li_2. The open squares represent the experimental data, while the solid (red) lines are the smeared out step functions fitted to the data. The scatter at the baseline is mainly due

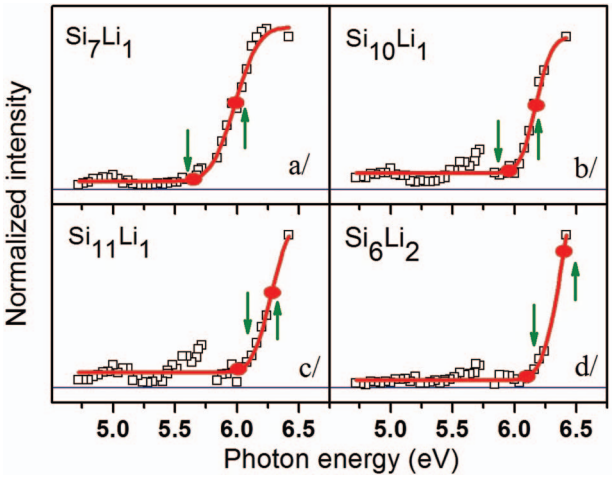

FIG. 2. PIE curves of the Si_nLi_m clusters ($n \leq 11$ and $m = 1, 2$) with an AIE below 6.25 eV; Si_7Li, $Si_{10}Li$, $Si_{11}Li$, and Si_6Li_2. The open squares represent the experimental data, while the solid red lines represent smeared-out step functions fitted to the data. The experimental VIE and the ionization threshold are both indicated by a red dot. The positions of the calculated VIE and AIE are indicated by green arrows.

to the low signal to noise ratio. The scatter above the VIE is intrinsic. The experimental VIE and the ionization thresholds are both indicated in the figures with a (red) dot. The positions of the VIEs and AIEs calculated in this work (described in Sec. IV) are indicated by green arrows. The small features in front of the ionization thresholds are parts of the PIE curves of $Si_{n-1}Li_{1,2+4}$ species which have the same mass as $Si_nLi_{1,2}$ and are probed at slightly higher lithium contents in the source.

III. COMPUTATIONAL METHODS

Electronic structure calculations are carried out using the GAUSSIAN 03 package.[38] The popular hybrid B3LYP functional in combination with the 6-311+G(d) basis set is used for optimizing geometries. Harmonic vibrational frequencies are calculated at this level to identify the obtained structures as local minima on the potential energy surface and to evaluate zero-point energy corrections. The B3LYP functional has shown to be good in predicting IEs of bare silicon clusters.[39–42] To obtain more accurate geometrical and energetic parameters, higher levels of theory such as the composite G3B3 method and coupled-cluster theory are used. The G3B3(G3/B3LYP) approach is a variance of the GAUSSIAN 3 (G3) method.[43] This is a composite technique in which a sequence of molecular orbital calculations is performed to obtain an improved total electronic energy of a given molecular species. Relative to the original G3 method, the equilibrium structure in the G3B3 theory is determined at the B3LYP/6-31G(d) level, instead of at the MP2/6-31G(d) level. Harmonic vibrational frequencies are computed at the same B3LYP level and scaled by a factor of 0.96 to take the known deficiencies at this level for this property into account. The scaled vibrational frequencies also give the zero-point energies (ZPEs) that are used for zero-point corrections to the total energies. The coupled-cluster CCSD(T) theory is used in conjunction with the correlation consistent aug-cc-pVTZ basis set for the small Si_nLi_m ($n = 2$–5 and $m = 1$–2) clusters. For larger Si_nLi_2 clusters ($n = 6$–11), single-point electronic energies are calculated at the CCSD(T)/aug-cc-pVDZ level for selected isomers using the B3LYP optimized geometries.

The AIE is calculated as the difference of the electronic energies, corrected by zero-point energies, of each neutral isomer and its corresponding cation having the similar shape. The cationic structure is obtained by optimizing from the neutral structure after removing an electron. For each isomer considered, a couple of neutral and cationic structures having similar shapes are located. The VIE is computed from the single-point electronic energy of the neutral and cationic forms at the optimized neutral geometry. The zero-point energies used in the IE values at the CCSD(T) level are taken from the B3LYP/6-311+G(d) harmonic vibrational frequencies.

In this study, the generation of new structures for each Si_nLi_m cluster system is initially based on the structures previously reported in the literature. Wang *et al.*[21] showed that the Si_nLi geometric structures are similar to those of corresponding anionic Si_n^- clusters, if one neglects the Li atom. On this basis, we generated structures of Si_nLi by adding a Li atom at different positions around the well-known geometric structures of the bare anionic silicon Si_n^- clusters and then optimize their geometries. Similarly, we create the new initial structures of Si_nLi_2 by adding the second Li atom around the different isomeric structures of Si_nLi. Besides, we also carried out systematic exchanges of the Si atoms by Li atoms in order to derive additional structures for both series of Si_nLi and Si_nLi_2 clusters. Finally, the natural charges of atoms are computed using the NBO5.G code[44] integrated into the GAUSSIAN 03 suite. (See Tables S1–S8 in the supplementary material.[45])

IV. RESULTS AND DISCUSSION

This part is organized in three sections. In the first section we discuss the structures and energetics of lower-lying isomers of each cluster size for both neutral and cationic $Si_nLi_m^{0/+}$ with $n = 2$–11 and $m = 1$–2. The second and third sections are devoted to their growth mechanism and their dissociation energies, respectively. Conventionally, the **n-mX$^{0/+}$** label is used for the isomers of the $Si_nLi_m^{0/+}$ cluster, with **X** = **A**, **B**, **C**... referring to the different isomers with increasing relative energy.

A. Structures of $Si_nLi_m^{0/+}$ with $n = 2$–11 and $m = 1, 2$

1. $Si_nLi_m^{0/+}$ with $n = 2$–5 and $m = 1, 2$

The calculated geometries of the smallest lithium doped silicon clusters, Si_nLi_m with $n = 2$–5 and $m = 1, 2$, are displayed in Fig. 3. The lowest energy isomers agree well with the results reported in previous theoretical studies.[21–24] In particular, Sporea *et al.*[26] investigated their structures and IEs at the B3LYP/6-31+G(d) level. Wang *et al.*[21] performed calculations using the quadratic configuration interaction method, QCISD/6-311+G(d)//MP2/6-31G(d), for the small neutral clusters Si_nLi ($n = 2$–7) and found a correlation between

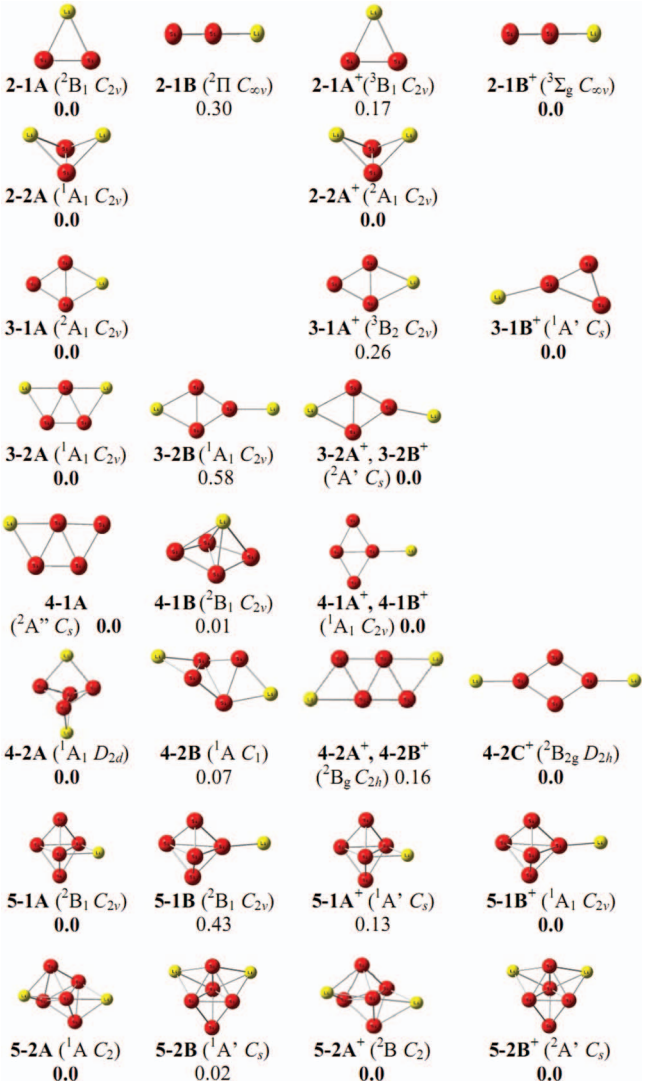

FIG. 3. Low-lying isomers of neutral and cationic $Si_nLi_m^{0/+}$ with $n = 2$–6 and $m = 1, 2$. The entries are electronic state, point group, and relative energy (in eV, calculated at the B3LYP/6-311+G(d)+ZPE level).

vertical IEs of Si_nLi and electron affinities of the corresponding Si_n clusters.

Table I presents the calculated AIEs and VIEs of the lowest energy isomers found for Si_nLi_m at three different levels of theory including B3LYP/6-311+G(d), G3B3, and CCSD(T)/aug-cc-pVTZ. For these small clusters, the lowest energy isomers in both neutral and cationic forms have the same shape (labeled by the letter **A**). The AIE and VIE values obtained using B3LYP slightly differ from those derived at CCSD(T) with the deviations being smaller than ±0.1 eV. Also, the differences with the G3B3 values are less than ±0.1 eV, except for **4-2A** where differences between B3LYP and G3B3 of more than 0.3 and 0.2 eV are found for the AIE and VIE values, respectively. Accordingly, the B3LYP approach is considered to be reliable to investigate the ionization energies of the larger Si_nLi_m clusters, with an uncertainty of about ±0.1 eV relative to CCSD(T) values.

2. $Si_6Li_m^{0/+}$ with m = 1, 2

The isomeric structures of Si_6Li and Si_6Li_2 and their cations are illustrated in Fig. 4. The C_{2v} pentagonal bipyramid **6-1A** in a $^2B_2$ state is the lowest-lying form of the neutral Si_6Li. This is in agreement with the results of Yang *et al.*[23] The cation **6-1A+** with a similar shape to the neutral is a local minimum lying 0.18 eV above the lowest-lying C_s isomer **6-1B+**. The Li atom in the cationic isomer **6-1B+** binds with a Si atom, whereas in the neutral **6-1A** the dopant adds on the surface of the silicon framework. The mass spectra in Fig. 1 indicate that the ionization threshold of Si_6Li is higher than 6.42 eV, which is closer the computed AIE value for isomer **6-1A** (6.41/6.12 eV at B3LYP/CCSD(T), see Table II) than that for isomer **6-1B** (AIE of 5.59/5.45 eV at B3LYP/CCSD(T)).

For Si_6Li_2, the two lowest-lying isomers **6-2A** and **6-2B** are energetically degenerate according to the B3LYP calculations. The CCSD(T) results show a marginal preference for **6-2B** by only 0.01 eV. The degeneracy of both isomers can be related to the similar silicon framework in which the Li atoms play the role of charge donor. They both have one Li atom situated on a pentagon and the other Li capped on different Si−Si edges.

The experimental PIE curve of Si_6Li_2 (see Fig. 2(d)) yields an ionization threshold energy of 6.10 ± 0.26 eV and a VIE of 6.40 ±0.15 eV, in good agreement with the calculated values of **6-2A,** being 6.15/6.00 eV and 6.47/6.34 eV for the AIE and VIE at the B3LYP/CCSD(T) level, respectively. The AIE and VIE values of **6-2B** are somewhat lower than the

TABLE I. AIE and VIE of the lowest energy isomers of Si_nLi_m clusters with $n = 2$–5 and $m = 1$–2 calculated at three different levels of theory.

	B3LYP/6-311+G(d)		G3B3		CCSD(T)/aug-cc-pVTZ	
Ionization transition	AIE (eV)	VIE (eV)	AIE (eV)	VIE (eV)	AIE (eV)	VIE (eV)
2-1A(^{2}B$_1$) → **2-1A**$^+$(^{3}B$_1$)	6.79	6.89	6.83	6.93	6.85	6.96
3-1A(^{2}A$_1$) → **3-1A**$^+$(^{3}B$_2$)	6.95	7.27	6.96	7.22	6.85	7.18
4-1A(^{2}A″) → **4-1A**$^+$(^{1}A$_1$)	6.09	6.24	6.21	6.29	6.09	6.22
5-1A(^{2}B$_1$) → **5-1A**$^+$(^{1}A′)	6.62	7.41	6.73	7.25	6.62	7.40
2-2A(^{1}A$_1$) → **2-2A**$^+$(^{2}A$_1$)	6.01	6.18	6.08	6.23	5.94	6.14
3-2A(^{1}A$_1$) → **3-2A**$^+$(^{2}A′)	6.29	6.61	6.37	6.69	6.27	6.60
4-2A(^{1}A$_1$) → **4-2A**$^+$(^{2}B$_g$)	5.79	6.83	6.13	7.05	5.85	6.86
5-2A(^{1}A) → **5-2A**$^+$(^{2}B)	6.37	6.83	6.46	6.93	6.37	6.86

TABLE II. Calculated and experimental values of AIEs and VIEs of Si_nLi and Si_nLi_2 neutral clusters with $n = 6$–11.[a]

	AIE (eV)			VIE (eV)		
Ionization process	B3LYP	CCSD(T)	Exp.	B3LYP	CCSD(T)	Exp.
6-1A($^2B_2$) → 6-1A$^+$($^1A_1$)	6.41	6.12	6.42–7.89	6.94	6.70	
6-1B($^2B_1$) → 6-1B$^+$($^1A'$)	5.59	5.45		6.44	6.19	
6-2A($^1A_1$) → 6-2A$^+$(^1A)	6.15	6.00	6.10 ± 0.26	6.47	6.34	6.40 ± 0.15
6-2B($^1A'$) → 6-2B$^+$($^2A'$)	6.01	5.90		6.22	6.12	
6-2C($^1A_1'$)→ 6-2C$^+$($^2A'$)	6.84	6.80		7.08	7.13	
6-2D($^1A'$) → 6-2D$^+$($^2A''$)	6.09	5.89		6.48	6.38	
7-1A($^2B_1$) → 7-1A$^+$($^1A_1$)	5.60	5.45	5.65 ± 0.04	6.06	5.87	5.98 ± 0.01
7-1B($^2A''$) → 7-1B$^+$(^1A)	6.24	6.05		6.57	6.45	
7-2A($^1A_1$) → 7-2A$^+$(^2A)	6.48	6.41	6.20–6.42	6.72	6.71	
7-2B(^1A) → 7-2B$^+$(^2A)	6.07	5.98		6.33	6.31	
7-2C(^1A) → 7-2C$^+$(^2A)	5.95	5.91		6.35	6.33	
7-2D($^1A_1$) → 7-2D$^+$(^2A)	5.25	5.20		5.74	5.65	
8-1A($^2A''$) → 8-1A$^+$(^1A)	6.60	6.42	<6.42	7.12	6.95	
8-1B(^2A) → 8-1B$^+$(^1A)	6.10	5.94		6.43	6.33	
8-1C(^2A) → 8-1C$^+$(^1A)	6.41	6.29		6.83	6.67	
8-1D(^2A) → 8-1D$^+$(^1A)	5.68	5.43		6.05	5.88	
8-2A($^1A'$) → 8-2A$^+$($^2A'$)	6.87	6.89	6.42–7.89	7.03	6.99	
8-2B($^1A_1$) → 8-2B$^+$($^2A_2$)	6.49	6.41		6.74	6.70	
9-1A(^2A)→ 9-1A$^+$(^1A)	5.91	5.68	<7.89	6.53	6.38	
9-1B(^2A) → 9-1B$^+$(^1A)	5.71	5.42		6.28	6.07	
9-2A(^1A) → 9-2A$^+$(^2A)	6.36	6.27	6.42–7.89	6.72	6.73	
9-2B($^1A'$) → 9-2B$^+$(^2A)	6.43	6.37		6.76	6.80	
9-2C($^1A'$)→ 9-2C$^+$(^2A)	6.26	6.21		6.53	6.52	
9-2D(^1A)→ 9-2D$^+$(^2A)	6.36	6.25		6.72	6.70	
10-1A($^2A'$) → 10-1A$^+$($^1A'$)	5.86	5.61	5.95±0.05	6.19	6.00	6.17±0.01
10-1B($^2A'$) → 10-1B$^+$(^1A)	5.80	5.53		6.24	6.06	
10-1C($^2A'$) → 10-1C$^+$(^1A)	5.84	5.64		6.36	6.20	
10-1D($^2A'$) → 10-1D$^+$(^1A)	5.82	5.56		6.18	6.00	
10-2A(^1A) → 10-2A$^+$($^2A'$)	6.01	6.07	<7.89	6.77	6.66	
10-2B($^1A'$) → 10-2B$^+$($^2A'$)	5.95	6.09		6.75	6.63	
10-2C(^1A)→ 10-2C$^+$(^2A)	5.99	6.01		6.74	6.61	
10-2D(^1A) → 10-2D(^2A)	5.81	5.73		6.29	6.27	
11-1A(^2A) → 11-1A$^+$(^1A)	5.96	5.79	6.01±0.16	6.89	6.76	>6.20
11-1B($^2A'$) → 11-1B$^+$(^1A)	6.10	5.87		6.47	6.27	
11-1C($^2A'$)→ 11-1C$^+$(^1A)	5.83	5.83		6.46	6.26	
11-1D(^2A) → 11-1D$^+$($^1A'$)	5.63	5.47		6.38	6.17	

[a]Calculated AIEs are corrected by ZPEs obtained at the B3LYP/6-311+ G(d) level.

experimental values, being 6.01/5.90 eV and 6.22/6.12 eV for the AIE and VIE at B3LYP/CCSD(T). But, given the experimental and theoretical uncertainties on the derived values, the presence of isomer **6-2B** in the cluster beam cannot definitely be excluded.

3. $Si_7Li_m^{0/+}$ with m = 1, 2

For these systems, our results concur with previous studies[21,23] that the most stable structure of Si_7Li is an edge-capped pentagonal bipyramid where the Li takes the capping position. Other isomers of this cluster have not been discussed in earlier studies. Fig. 4 illustrates the lower-lying isomers of $Si_7Li^{0/+}$ and $Si_7Li_2^{0/+}$. Of particular interest is the observation that the substitutive isomer **7-1B** in which the Li atom substitutes a Si atom of the pentagon is only 0.16 eV higher in energy than **7-1A**.

The most stable cation of Si_7Li^+, **7-1A$^+$**, exhibits a structure similar to the neutral ground state. The substitutive isomer **7-1B$^+$**, however, becomes much less stable than **7-1A$^+$**.

The doubly lithium doped neutral Si_7Li_2 cluster adopts **7-2A**, a bicapped pentagonal bipyramid, as its lowest energy form. In this isomer, both Li atoms substitute Si atoms of the pentagon. **7-2D**, where both Li atoms adsorb to edges of the pentagon, is 0.51 eV higher in energy than **7-2A**. However, there is again a reversed energy ordering for the $Si_7Li_2^+$ cation, namely, **7-2D$^+$** becomes the lowest-lying isomer being 0.72 eV more stable than **7-2A$^+$**.

The experimental PIE curve of Si_7Li (Fig. 2(a)) yields an ionization threshold energy of 5.65 ± 0.04 eV and a VIE of 5.98 ± 0.01 eV. The calculated B3LYP values for **7-1A** of 5.60 and 6.06 eV, respectively, agree well with the experiment. Calculated AIE and VIE for isomer **7-1B** are significantly higher than the experimental values (see Table II).

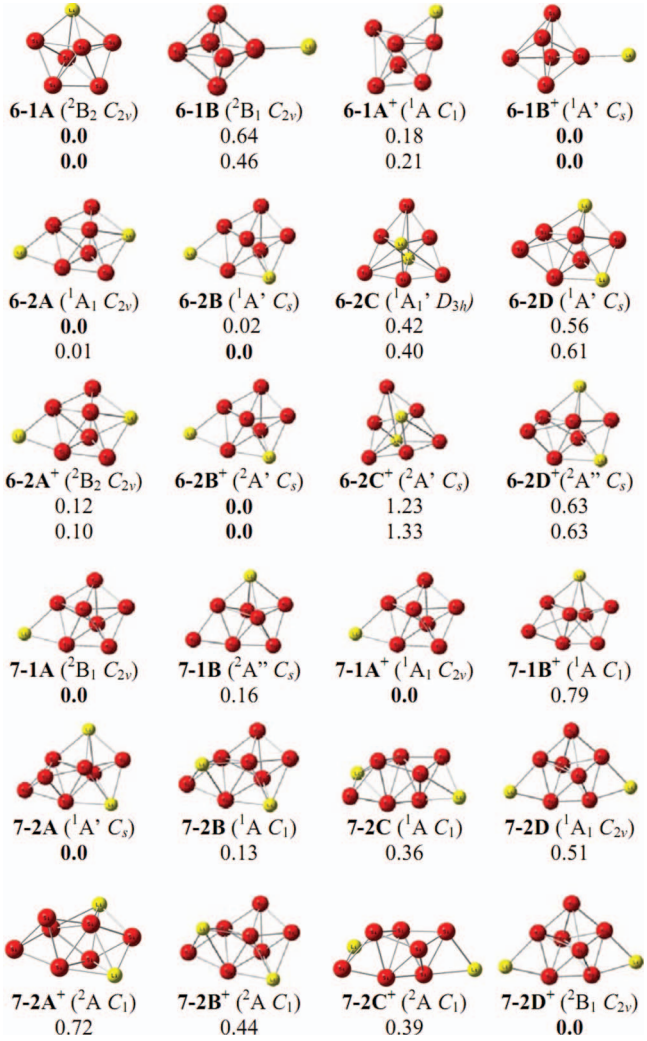

FIG. 4. Low-lying isomers of the neutral and cationic $Si_6Li_m^{0/+}$ and $Si_7Li_m^{0/+}$ with $m = 1, 2$. Relative energies (in eV) are calculated at the B3LYP/6-311+G(d) + ZPE (upper) and CCSD(T)/aug-cc-pVTZ + ZPE (lower) level.

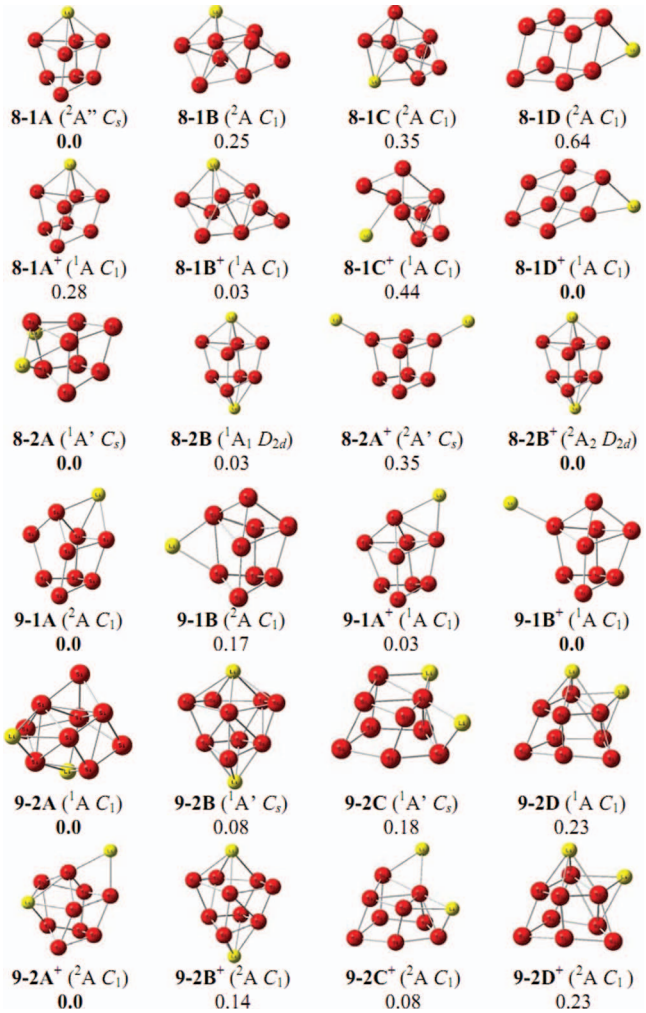

FIG. 5. Low-lying isomers of the neutral and cationic $Si_8Li_m^{0/+}$ and $Si_9Li_m^{0/+}$ with $m = 1, 2$. Relative energies (in eV) are calculated at the B3LYP/6-311+G(d) + ZPE level.

Therefore, **7-1A** is likely the isomer present in the experiment. No accurate value for the ionization threshold could be determined in the experiment, but mass spectra obtained by ionization with 6.42 eV laser light show that the ionization threshold must be between 6.24 and 6.42 eV. This result supports **7-2A** and excludes **7-2D** as the global minimum of this size.

4. $Si_8Li_m^{0/+}$ with $m = 1, 2$

The global minimum **8-1A** of Si_8Li (Fig. 5) can, on the one hand, be considered as a substitutive derivative of the C_{2v} symmetric bicapped pentagonal bipyramid Si_9 (cf., Refs. 40 and 41) and keeps the C_{2v} symmetry of Si_9. On the other hand, **8-1A** can be formed by adding Li^+ on Si_8^-.[41] **8-1D**, which is composed of bicapped Si_8^- and Li^+, is 0.64 eV higher in energy than **8-1A**. Conversely, the cationic system Si_8Li^+ favors the additive isomer **8-1D$^+$**, which becomes the lowest-lying isomer. Again, a reversed energy ordering is found following electron removal at the expense of substitutive derivatives such as **8-1A$^+$**.

Si_8Li_2 has two very close-lying isomers **8-2A** and **8-2B**, both of which have a Si framework similar to that of the dianion Si_8^{2-}.[19] The positions of the Li atoms in **8-2A** and **8-2B** are also of substitutive type as compared to the bare Si_9 cluster. The cationic isomer **8-2B$^+$** turns out to be the ground state of $Si_8Li_2^+$. In the cation, the Li atoms stay further from the Si framework than in the neutral.

No accurate experimental value for the ionization threshold could be determined either for the monolithiated or dilithiated cluster. However, the recorded mass spectra indicate that the ionization threshold of Si_8Li is below 6.42 eV, whereas that of Si_8Li_2 is between 6.42 and 7.89 eV. This is in agreement with the calculated higher AIE of Si_8Li_2 than Si_8Li, but does not allow making a definite assignment of their ground state structures.

5. $Si_9Li_m^{0/+}$ with $m = 1, 2$

The neutral Si_9Li system (Fig. 5) has **9-1A** as the global minimum. In this isomer, the Li atom adds on a face of the bicapped pentagonal bipyramid Si_9.[40,41] **9-1B**, an edge-capped derivative of Si_9, is located only 0.17 eV higher in energy

than **9-1A**. This means that face-capping is slightly preferred over edge-capping for the neutral state of this cluster. In the cationic Si_9Li^+, three close-lying isomers are generated by capping Li at different positions on a silicon framework similar to the ground state of the anionic Si_9^-.[41] This suggests that the Li^+ cation loosely moves around a silicon frame. Among these isomers, **9-1B+** where Li^+ only binds to one Si atom constitutes the most stable isomer.

For the doubly lithium doped system, the lowest-lying isomer **9-2A** is a penta-capped trigonal prism in which one Li atom substitutes a Si position of the trigonal prism of Si_{10} (Refs. 40 and 41) and the other Li atom adds on a side face. **9-2B**, being only 0.08 eV less stable than **9-2A**, is also based on the tetra-capped trigonal prism shape of Si_{10}, but one Li atom now takes a substitutive position and the other takes a bridging position. Both Li atoms in **9-2C** and **9-2D** have additive positions. For the $Si_9Li_2^+$ cation, we find **9-2A+** as the lowest-lying isomer. However, **9-2C+**, which becomes quasi-degenerate with **9-2A+**, still has the bicapped pentagonal bipyramidal shape of Si_9 (Ref. 40), and both Li atoms are added around the silicon framework. **9-2D+** remains characterized by the shape of Si_9, with Li atoms circulating around, but this isomer lies energetically higher than the former.

Due to the presence of Si_8Li_5 in the cluster beam, of which the maximum in the isotopic distribution (259 amu) coincides with that of Si_9Li, it was hard to experimentally determine an ionization threshold for Si_9Li. At least no sharp photoionization curve could be recorded. Also, for Si_9Li_2 no accurate experimental value for the ionization threshold could be determined. Based on the mass spectra collected by ionization with 6.42 and 7.89 eV laser light, it is known that the ionization threshold must be larger than 6.42 and below 7.89 eV. Of the four lowest energy isomers for Si_9Li_2, this does only excludes **9-2C**.

6. $Si_{10}Li_m^{0/+}$ with m = 1, 2

Fig. 6 illustrates the shape, symmetry, and energetics of the lower-lying structures of $Si_{10}Li_{1,2}^{0/+}$. All the four lower-lying isomers of $Si_{10}Li$ have the tetra-capped trigonal prism framework of Si_{10} (Refs. 40 and 41) with the Li atom exohedrally adds on different positions. In a previous paper, Sporea and Rabilloud[46] found that a Li atom can be encapsulated in the silicon cage Si_{10}. The lowest-lying isomer c-Li@Si_{10}, which possesses D_{4d} symmetry of lithium-doped cage-like silicon clusters, however, is calculated to be 1.5 eV higher in energy than **10-1A**. This shows that lithium prefers to expose on the surface of the silicon cores.

A similar structure to the global minimum of neutral **10-1A** is found for the cationic $Si_{10}Li^+$, **10-1A+**, but it is slightly less stable than **10-1B+** which has an edge-capped lithium on the Si_{10} tetra-capped trigonal prism. The face-capped **10–1A+** (+0.01 eV) and top-capped **10-1C+** (+0.06 eV) isomers are nearly degenerate.

Regarding the doubly doped species, the lowest-lying isomer **10-2A** contains a bicapped square antiprism Si_{10} framework, similar to the ground state structure of the dianionic Ge_{10}^{2-} as found by King *et al.*,[47] and has two face-capping Li atoms. The higher energy isomers **10-2B** and **10-2C** differ from **10-2A** only by the positions of the capping Li atoms. It seems that the bicapped square antiprism Si_{10}^{2-} is rather stable, and Li atoms mainly are electron donors interacting by electrostatic forces and moving as Li^+ cations around the silicon dianion. The **10-2D** isomer, where the tetra-capped trigonal prism remains and the Li atoms add on different faces, is also energetically close to **10-2A**. It should be noted that for this size more isomers are found to be close in energy, which implies a large spectrum of isomers having similar energy content. Different from the neutral $Si_{10}Li_2$, the cationic $Si_{10}Li_2^+$ clusters prefer the tetra-capped trigonal prism framework of Si_{10}. The three lowest-lying isomers including **10-2D+** (0.0 eV), **10-2A+** (+0.03 eV), and **10-2B+** (+0.07 eV) have the Li atoms at different positions around that silicon frame.

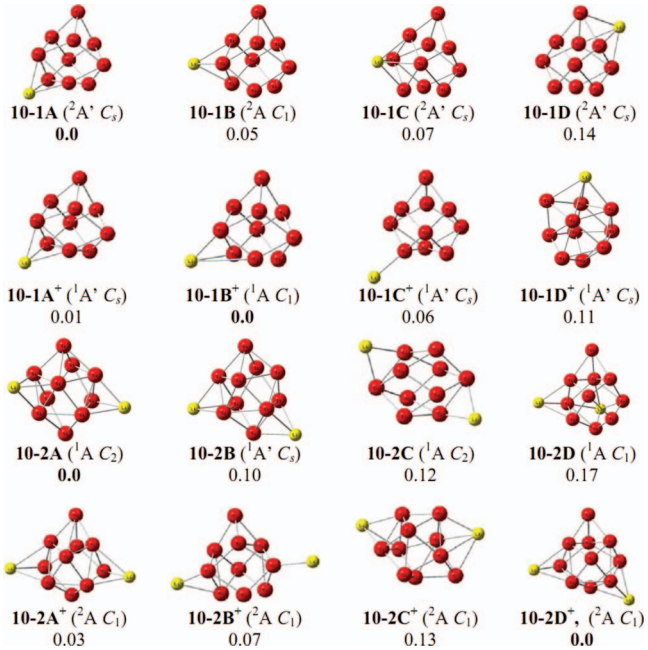

FIG. 6. Low-lying isomers of the neutral and cationic clusters $Si_{10}Li_m^{0/+}$ with $m = 1, 2$. Relative energies (in eV) are calculated at the B3LYP/6-311+G(d) + ZPE level.

Fig. 2(b) shows the PIE curve of $Si_{10}Li$. The experiment yields an ionization threshold energy of 5.95 ± 0.05 eV and a VIE of 6.17 ± 0.01 eV. The B3LYP values for **10-1A** of 5.86 and 6.19 eV, respectively, compare favorably with experiment. However, the other isomers shown in Fig. 8 cannot be fully excluded. No ionization threshold could be measured for the dilithiated system. But based on the appearance of the $Si_{10}Li_2$ in the mass spectrum taken after ionization with 7.89 eV photons, it is clear that the ionization threshold must be lower than this value.

7. $Si_{11}Li_m^{0/+}$ with m = 1, 2

The calculated results for this system are summarized in Fig. 7. **11-1A**, which is a substitutive derivative of a penta-capped trigonal prism structure, is the lowest-lying isomer of $Si_{11}Li$ using B3LYP. However, CCSD(T) suggests that **11-1C**

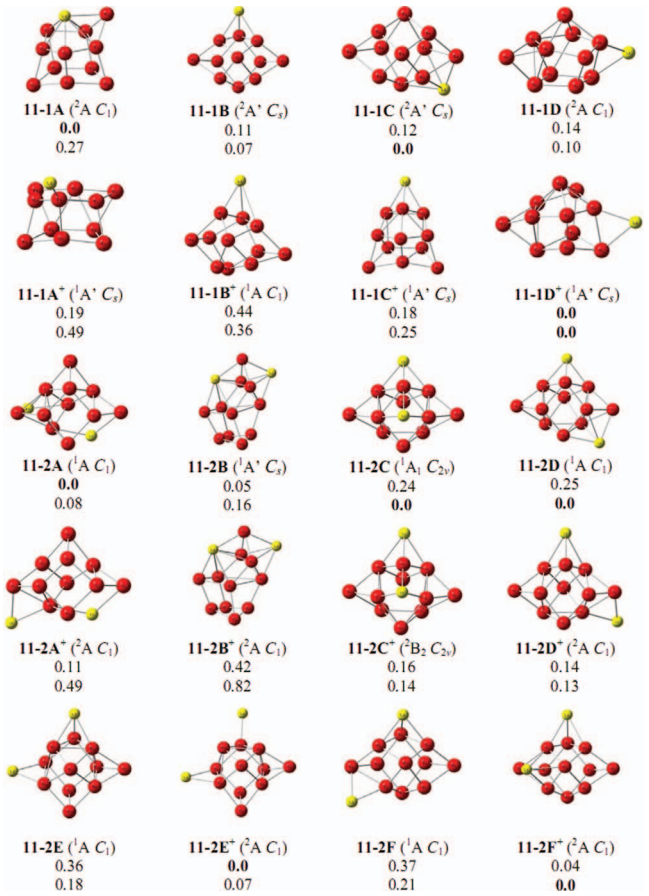

FIG. 7. Low-lying isomers of the neutral and cationic clusters $Si_{11}Li_m^{0/+}$ with $m = 1$–2. Relative energies (eV) are calculated at the B3LYP/6-311+G(d) + ZPE (upper values) and CCSD(T)/ aug-cc-pVTZ + ZPE (lower values).

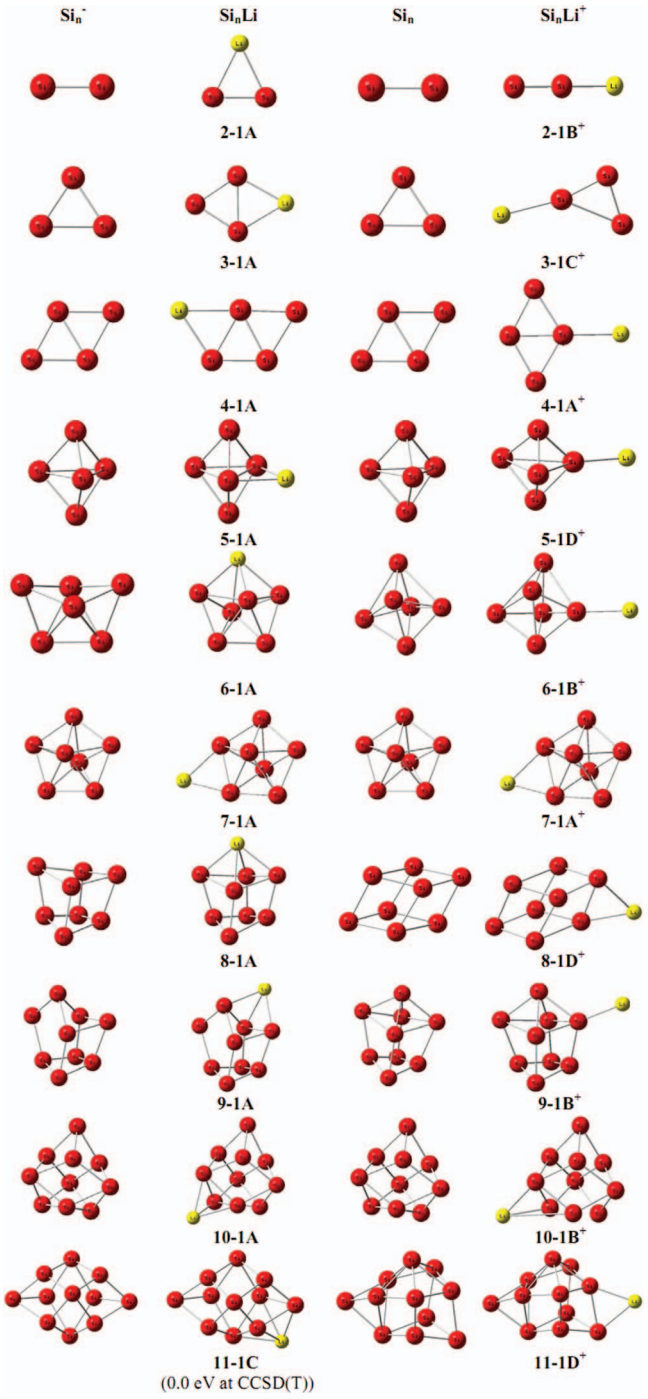

FIG. 8. The growth pattern of the neutral and cationic Si_nLi systems compared with Si_n^- and Si_n ground state structures. Geometries of the bare Si clusters are taken from Refs. 39, 40, and 43 and reoptimized at the B3LYP/6-311+G(d) level.

is the most stable structure and its geometric shape of silicon framework is similar to that of the most stable Si_{11}^- anionic isomer.[48] This agrees with a previous finding that the geometric shapes of Si_nLi are similar to those of the corresponding Si_n^- anions if we neglect the Li atom in Si_nLi.[21] **11-1B** and **11-1C** are formed by adding Li on different positions of the penta-capped trigonal prism Si_{11}. The cationic isomer **11-1D+**, which is found to be the most stable form of the $Si_{11}Li^+$, is, in fact, an edge-capped Si_{11}. The Si_{11} framework of this isomer is geometrically similar to the ground state of the neutral Si_{11} cluster.[40,42]

Fig. 2(c) shows the PIE curve of $Si_{11}Li$. The experiment yields an ionization threshold energy of 6.01 ± 0.16 eV and a VIE above 6.20 eV. Accordingly, our B3LYP values for **11-1A** of 5.96 and 6.89 eV, respectively, are comparable with the experiment. Calculated AIE values for isomers **11-1C** and **11-1D** are significantly below 6.01 eV, excluding them as ground state structures. However, based on the calculated ionization energies, isomer **11-1B** cannot be ruled out.

Based on the B3LYP calculations, the lowest energy isomer **11-2A** of $Si_{11}Li_2$ has the shape of hexa-capped trigonal prism and one Li atom substitutes a Si position of the trigonal prism of Si_{12} (Ref. 40), whereas the other Li atom adds on different face. According to the CCSD(T) results, however, both isomers **11-2C** and **11-2D** which are energetically degenerate are the most stable isomers and they both are only 0.08 eV lower in energy than **11-2A**. Structurally, the **11-2C** and **11-2D** also have the hexa-capped trigonal prism framework of Si_{12} (Ref. 40) in which one Li atom substitutes a capped Si position and the other Li atom adds on different positions. In contrast, the B3LYP predicts that the cation $Si_{11}Li_2^+$ adopts **11-2E+** as its most preferred form where both Li atoms bind on the surface of the silicon framework. However, **11-2F+**

becomes the most stable isomer at the CCSD(T) level. **11-2F+** has both Li atoms added on two surfaces of silicon core of the most stable Si_{11}^- anion.[48]

B. Growth mechanisms of $Si_nLi_m^{0/+}$

Based on the comparison between the available experimental ionization energies and the calculated values for $Si_nLi_{1,2}$, it is reasonable to assume that the lowest energy isomers located at the B3LYP level are the isomers that are present in the experiment (at least none of the lowest energy isomers found could be excluded on the basis of this comparison). From here on, we therefore focus on the lowest energy isomers found for $Si_nLi_{1,2}^{0/+}$ and analyze their growth patterns.

To facilitate the comparison, Figs. 8 and 9 summarize the ground state structures of Si_nLi, Si_nLi^+, Si_nLi_2, and $Si_nLi_2^+$ with $n = 2$–11 and compare them with those of the bare clusters Si_n^-, Si_n, and Si_{n+1} whose structures are taken from previous studies[40,41,48] and reoptimized at the B3LYP/6-311+G(d) level. We find that the Li dopant atoms adopt quite different behaviors depending on the number of Li atoms and on the charge state.

In the singly doped neutral Si_nLi clusters, the Li atom favors addition on either an edge or a face of a Si_n framework that is similar to the ground state structure of the anionic Si_n^-. In some cases, the additive position can alternatively be described as substituting a silicon atom in Si_{n+1}, such as in Si_5Li, Si_6Li, Si_8Li, and $Si_{10}Li$. Generally, if the Li atom is located at the additive positions, it preferentially chooses a position which is also a substitution to the corresponding Si_{n+1} framework.

For the cations Si_nLi^+, Li seems to either bind with one Si atom of the bare Si_n cluster or adds on one of its edges. There is no exception on this empirical rule in the size range $n = 2$–11. In the positive charged state, the Li atom moves more freely due to the less negative charge distribution on the silicon frame; therefore, it has fewer bonds with the silicon atoms than in the neutral.

Fig. 9 shows that the doubly doped Si_nLi_2 species bear the shape of the Si_{n+1} counterparts. One Li atom actually substitutes into a Si position of Si_{n+1}, whereas the other Li atom is adding on an edge or a face. $Si_{10}Li_2$ is an exception on this observation. The ground state of $Si_{10}Li_2$ has both Li atoms added on the surface of the dianionic Si_{10}^{2-}.[49] This is due to the high stability of the dianion counterpart. The substitution mechanism appears to persist in the doubly doped system, in particular for the larger sizes.

In contrast to the neutrals, the $Si_nLi_2^+$ cations have both Li atoms being added on an edge or a face of the Si_n^- framework. Again, the substitution is disfavored in this charged state.

Concerning the charge distribution, the natural net charges of the atoms on the lowest-lying Si_nLi clusters are listed in Table S9 of the supplementary material.[45] The Li atom consistently has a large positive charge; the charge transfer from Li to the Si_n amounts from 0.7 in SiLi up to 0.9 electron in $Si_{11}Li$. Thus, the charge transfer from the alkali metal atom to the silicon core is nearly complete, irrespectively of the cluster size.

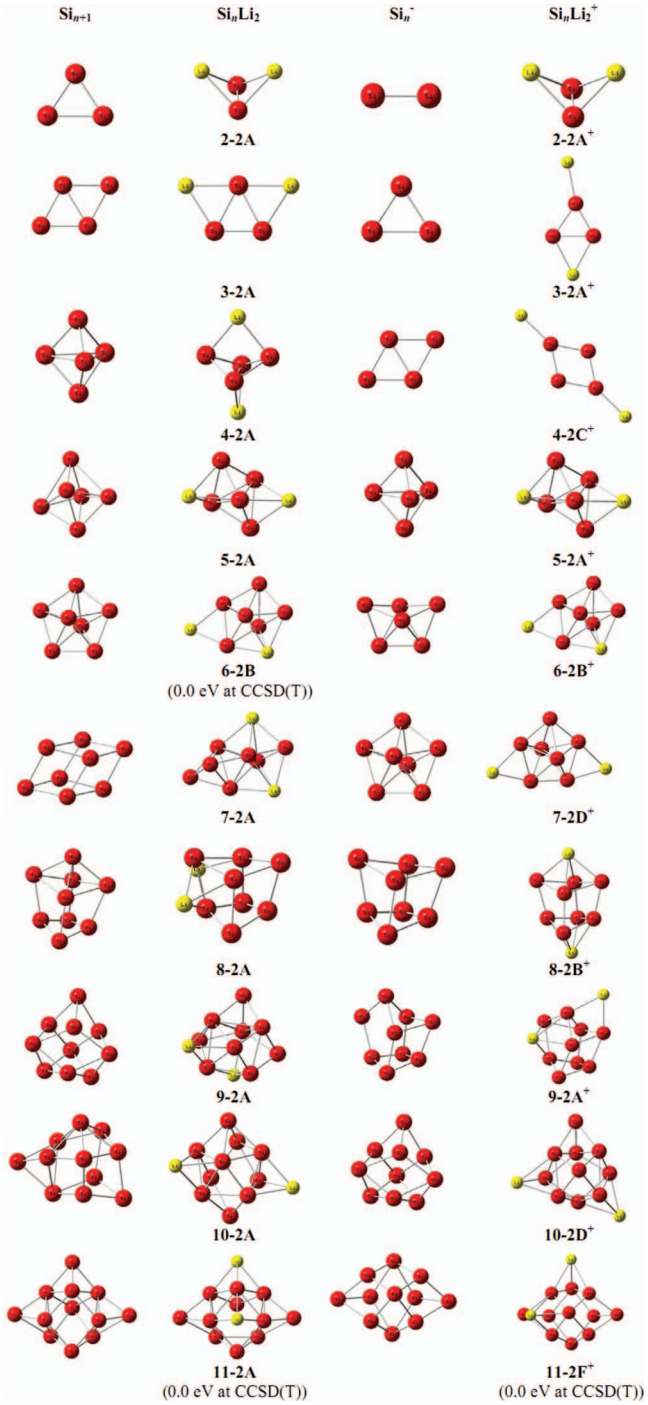

FIG. 9. The growth pattern of the neutral and cationic Si_nLi_2 systems. Geometries of the bare Si clusters are taken from Refs. 39, 40, and 43 and reoptimized at the B3LYP/6-311+G(d) level.

C. Dissociation energies

Dissociation energies of the Si_nLi and Si_nLi^+ with $n = 1$–11 clusters are calculated using the B3LYP/6-311+G(d) method for different fragmentation paths and illustrated in Fig. 10.

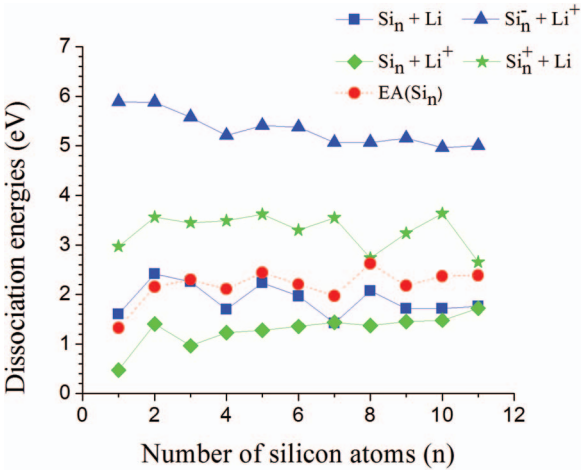

FIG. 10. Dissociation energies (corrected by ZPE) of Si_nLi ($Si_nLi \rightarrow Si_n + Li$ and $Si_nLi \rightarrow Si_n^- + Li^+$) and Si_nLi^+ ($Si_nLi^+ \rightarrow Si_n + Li^+$ and $Si_nLi^+ \rightarrow Si_n^+ + Li$) and the electron affinity of Si_n calculated using the B3LYP method as a function of the number of Si atoms.

The dissociation energy D_{e1} is defined as the energy required in the reaction $Si_nLi \rightarrow Si_n + Li$. This quantity has local minima for $n = 1$, 4, and 7 and is maximal for $n = 2$, 5, and 8. This means that SiLi, Si_4Li, and Si_7Li are relatively less stable and the Si_2Li, Si_5Li, and Si_8Li are relatively more stable Si_nLi clusters. It is interesting to note a remarkable similarity between the evolution of the dissociation energy D_{e1} of binary Si_nLi clusters and the electron affinity (EA) of bare Si_n with the size ($n = 1$–11). Both curves show local minima for $n = 1$, 4, and 7 and local maxima for $n = 5$ and 8 (see Fig. 10). This parallelism, which can be understood by the correspondence between the HOMO of Si_nLi and the LUMO of Si_n had already been noticed by Kishi *et al.*[29] and was verified by Sporea *et al.*[22] for small Si_nLi ($n = 3$–6). While the energy of the LUMO is relevant for the EA, the HOMO energy scales with the bond dissociation energy.

The D_{e2} values, which are defined as the energy required in the heterolytic bond cleavage reaction $Si_nLi \rightarrow Si_n^- + Li^+$, are also calculated. The size dependence of this heterolytic reaction path is not pronounced. Fig. 10 shows that all dissociation energies according to the $Si_nLi \rightarrow Si_n^- + Li^+$ process are much larger than those of the corresponding homolytic dissociation energies in the reaction $Si_nLi \rightarrow Si_n + Li$. This means that the homolytic bond cleavage is largely favored over the heterolytic processes.

D_{e3} and D_{e4} are defined as the energy required for the $Si_nLi^+ \rightarrow Si_n + Li^+$ and $Si_nLi^+ \rightarrow Si_n^+ + Li$ reactions, respectively. D_{e3} has a local minimum for $n = 3$ and local maxima for $n = 2$ and 11. The D_{e4} is local minima for $n = 6$, 8, and 11 and local maxima for $n = 2$, 7, and 10. The D_{e4} values are larger than D_{e3} for all Si_nLi^+ sizes. Accordingly, the Si_nLi^+ cations favor cationic Li^+ ejection over neutral Li elimination.

Proceeding in the opposite directions, namely, $Si_n^- + Li^+ \rightarrow Si_nLi$ and $Si_n + Li^+ \rightarrow Si_nLi^+$, the corresponding D_{e2} and D_{e3} values represent the lithium cation affinities (LiCAs) of the anionic and neutral bare Si clusters, respectively. It is obvious from Fig. 10 that the LiCAs of the charged species are much larger than those of the neutral counterparts. Similarly, the D_{e1} and D_{e4} values define the Li atom affinities (LiAs) of the neutral and cationic bare Si clusters, respectively. In this case, the charged species have consistently larger LiAs than the neutrals. This suggests that the electrostatic attraction plays an important role in the addition process of the dopant.

V. CONCLUDING REMARKS

In the present combined theoretical and experimental study, the geometric and electronic structures of both neutral and cationic Si_nLi_m clusters, with $n = 2$–11 and $m = 1$, 2, were determined using quantum chemical methods including the B3LYP/6-311+G(d), G3B3, and CCSD(T)/aug-cc-pVnZ (n = D,T) levels. It is found that the shape of the cationic isomers does not differ much from their corresponding neutrals isomers following ionization. However, in a number of cases a reversed energy ordering between isomeric forms occurs.

We also determine the AIEs and VIEs of the Si_nLi_m clusters. The calculated AIE and VIE values at the B3LYP/6/311+G(d) level of Si_6Li_2, Si_7Li, $Si_{10}Li$, and $Si_{11}Li$ compare quite well with the corresponding experimental results obtained using the photoionization efficiency measurements. These are the only clusters of the investigated Si_nLi_m ($n = 2$–11 and $m = 1$, 2) series for which the experimental ionization energies were found to be lower than 6.25 eV.

The growth mechanism of the singly and doubly lithium doped silicon clusters can be understood on the basis of the following empirical observations:

(i) In the neutral Si_nLi, the Li atom favors addition on either an edge or a face of the anionic Si_n^-, while in the cationic Si_nLi^+, it connects one Si atom of the bare Si_n cluster or adds on one of its edges.

(ii) The neutral Si_nLi_2 clusters have the shape of the Si_{n+1} counterparts. One Li atom adds on an edge or a face of it, whereas the other Li substitutes into a Si position of Si_{n+1}. This differs from the growth pattern of the cationic $Si_nLi_2^+$, where both Li atoms add on an edge or a face.

(iii) The neutral $Si_{11}Li$ and $Si_{10}Li_2$ and cationic $Si_9Li_2^+$ clusters represent exceptions with Li atoms behaving differently. Their different structures can, in part, be understood from the stability of the relevant core Si clusters.

ACKNOWLEDGMENTS

The authors thank the K. U. Leuven Research Council (GOA, IDO, and PDM programs), the Research Foundation—Flanders (FWO-Vlaanderen), and the Belgian Interuniversity Attraction Poles (IAP) research program for continuing support. H.T.L. acknowledges the Vietnamese Government (MOET Program 322).

[1]K. Raghavachari and V. Logovinsky, Phys. Rev. Lett. **55**, 2853 (1985).
[2]G. Pacchioni and J. Koutecký, J. Chem. Phys. **84**, 3301 (1986).
[3]W. L. Brown, R. R. Freeman, K. Raghavachari, and M. Schluter, Science **235**, 860 (1987).

[4]O. Cheshnovsky, S. H. Yang, C. L. Pettiette, M. J. Craycraft, Y. Liu, and R. E. Smalley, Chem. Phys. Lett. **138**, 119 (1987).
[5]C. B. Winstead, S. J. Paukstis, and J. L. Gole, Chem. Phys. Lett. **237**, 81 (1995).
[6]E. C. Honea, A. Ogura, C. A. Murray, K. Raghavachari, W. O. Sprenger, M. F. Jarrold, and W. L Brown, Nature **366**, 42 (1993).
[7]U. Röthlisberger, W. Andreoni, and M. Parrinello, Rev. Lett. **72**, 665 (1994).
[8]S. Li, R. J. Van Zee, W. Weltner, and K. Raghvachari, Chem. Phys. Lett. **243**, 275 (1995).
[9]K. M. Ho, A. A. Shvartsburg, B. Pan, Z. Y. Lu, C. Z. Wang, J. G. Wacker, J. L. Fye, and W. L. Brown, Nature **392**, 582 (1998).
[10]A. A. Shvartsburg, B. Liu, M. F. Jarrold, and K. M. Ho, J. Chem. Phys. **112**, 4517 (2000).
[11]X. Zhu and X. C. Zeng, J. Chem. Phys. **118**, 3558 (2003).
[12]W. Hellmann, R. G. Hennig, S. Goedecker, C. J. Umrigar, B. Delley, and T. Lenosky, Phys. Rev. B **75**, 085411 (2007).
[13]A. Fielicke, J. T. Lyon, M. Haertelt, G. Meijer, P. Claes, J. de Haeck, and P. Lievens, J. Chem. Phys. **131**, 171105 (2009).
[14]J. T. Lyon, P. Gruene, A. Fielicke, G. Meijer, E. Janssens, P. Claes, and P. Lievens, J. Am. Chem. Soc. **131**, 1115 (2009).
[15]V. T. Ngan, P. Grune, P. Claes, E. Janssens, A. Fielicke, M. T. Nguyen, and P. Lievens, J. Am. Chem. Soc. **132**, 15589 (2010).
[16]V. Kumar, in *Nanosilicon*, edited by V. Kumar (Elsevier, Amsterdam, 2007).
[17]N. Veldeman, P. Gruene, A. Fielicke, P. Claes, V. T. Ngan, M. T. Nguyen, and P. Lievens, "Endohedrally doped silicon clusters," in *The Handbook of Nanophysics: Clusters and Fullerenes*, edited by K. D. Sattler (CRC, Boca Raton, 2010).
[18]S. M. Beck, J. Chem. Phys. **87**, 4233 (1987).
[19]V. T. Ngan and M. T. Nguyen, J. Phys. Chem. A **114**, 7609 (2010)
[20]C. Majumder and S. K. Kulshreshtha, Phys. Rev. B **70**, 245426 (2004).
[21]H. Wang, W. C Lu, Z. S. Li, and Ch. C. Sun, J. Mol. Struct.: THEOCHEM **730**, 263 (2005).
[22]C. Sporea, F. Rabilloud, X. Cosson, A. R. Allouche, and M. Aubert-Frécon, J. Phys. Chem. A **110**, 6032 (2006).
[23]J. C. Yang, L. Lin, Y. Zhang, and A. F. Jalbout, Theor. Chem. Acc. **121**, 83 (2008).
[24]C. Sporea, F. Rabilloud, and M. Aubert-Frécon, J. Mol. Struct.: THEOCHEM **802**, 85 (2007).
[25]D. Hao, J. Liu, and J. Yang, J. Phys. Chem. A **112**, 10113 (2008).
[26]C. Sporea, F. Rabilloud, A. R. Allouche, and M. Frécon, J. Phys. Chem. A **110**, 1046 (2006).
[27]B. H. Boo, S. J. Kim, M. H. Lee, and N. Nishi, Chem. Phys. Lett. **453**, 150 (2008).
[28]W. Tiznado, N. Perez-Peralta, R. Islas, A. Toro-Labbe, J. M. Ugalde, and G. Merino, J. Am. Chem. Soc. **131**, 9426 (2009).
[29]R. Kishi, S. Iwata, A. Nakajima, and K. Kaya, J. Chem. Phys. **107**, 3056 (1997).
[30]R. Kishi, H. Kawamata, Y. Negishi, S. Iwata, A. Nakajima, and K. Kaya, J. Chem. Phys. **107**, 10029 (1997).
[31]D. Y. Zubarev, A. I. Bolydrev, X. Li, L. F. Cui, and L. S. Wang, J. Phys. Chem. A **109**, 11385 (2005).
[32]D. Y. Zubarev, N. Alexandrova, A. I. Boldyrev, X. Li, L. F. Cui, and L. S. Wang, J. Chem. Phys. **124**, 124305 (2006).
[33]O. Kostko, S. R. Leone, M. A. Duncan, and M. Ahmed, J. Phys. Chem. A **114**, 3176 (2010).
[34]J. De Haeck, S. Bhattacharyyra, H. T. Le, D. Debruyne, N. M. Tam, V. T. Ngan, E. Janssens, M. T. Nguyen, and P. Lievens, "Ionization energies and structures of lithium doped silicon clusters," J. Chem. Phys. (submitted).
[35]W. Bouwen, P. Thoen, F. Vanhoutte, S. Bouckaert, F. Despa, H. Weidele, R. E. Silverans, and P. Lievens, Rev. Sci. Instrum. **71**, 54 (2000).
[36]K. Fuke, K. Tsukamoto, F. Misaizu, and M. Sanekata, J. Chem. Phys. **99**, 7807 (1993).
[37]T. Bergmann and T. P. Martin, J. Chem. Phys. **90**, 2848 (1989).
[38]M. J. Frisch, G. W. Trucks, H. B. Schlegel *et al.*, GAUSSIAN 03, Revision B.04, Gaussian, Inc., Pittsburgh, PA, 2003.
[39]C. Bauschlicher, Chem. Phys. Lett. **246**, 40 (1995).
[40]S. Nigam, C. Majumder, and S. K. Kulshreshtha, J. Chem. Phys. **121**, 7756 (2004).
[41]J. C. Yang, W. G. Xu, and W. S. Xiao, J. Mol. Struct.: THEOCHEM **719**, 89 (2005).
[42]W. Qin, W. C. Lu, L. Z. Zhao, Q. J. Zang, C. Z. Wang, and K. M. Ho, J. Phys.: Condens. Matter **21**, 455501 (2009).
[43]A. G. Baboul, L. A. Curtiss, and P. C. Redfern, J. Chem. Phys. **110**, 7650 (1999).
[44]E. D. Glendening, J. K. Badenhoop, A. E. Reed, J. E. Carpenter, J. A. Bohmann, C. M. Morales, and F. Weinhold, NBO 5.G (Theoretical Chemistry Institute, University of Wisconsin, Madison, WI).
[45]See supplementary material at http://dx.doi.org/10.1063/1.3672164 for ten tables that list the total electronic energies, zero-point energies, and Cartesian coordinates of selected lower-lying isomers (Tables S1–S8), the NBO charges (Table S9), and the dissociation energies of neutral and cationic clusters.
[46]C. Sporea and F. Rabilloud, J. Chem. Phys. **127**, 164306 (2007).
[47]R. B. King, I. Silaghi-Dumitrescu, and M. M. Uta, Inorg. Chem. **45**, 4974 (2006).
[48]B. Li and Q. Xu, Phys. Status Solidi **241**, 990 (2004).
[49]A. D. Zdetsis, J. Chem. Phys. **127**, 244308 (2007).